

# Robust and computational efficient autopilot design: A hybrid approach based on classic control and genetic-fuzzy sliding mode control

A. R. Babaei, M. Mortazavi and M. B. Menhaj  
arbabaei@aut.ac.ir

Aerospace Engineering Department, Amirkabir University of Technology  
Tehran, Iran

## ABSTRACT

The purpose of this paper is developing an efficient flight control strategy in terms of time response characteristics, robustness with respect to both parametric uncertainties and un-modeled nonlinear terms, number of required measurements, and computational burden. The proposed method is based on combination of a classic controller as principal section of the autopilot and a multi-objective genetic algorithm-based fuzzy output sliding mode control (FOSMC). FOSMC not only modifies robustness of the classic controller against uncertainties and external disturbances, but also modifies its time response for wide range of commands. FOSMC is a single input-single output controller that is based on the system output instead of the system states. In this situation, the proposed autopilot does not require measurement of other variables and observer, and also it is practicable because of considerable reduction in rule inferences then computational burden. As a critical application, the proposed method is applied to design the altitude hold mode autopilot for an UAV which is non-minimum phase, uncertain, and nonlinear.

## NOMENCLATURE

<b>E</b>	output error vector
$e_i$	$i$ th output error
EA	evolutionary algorithm
$C_{**}$	a parameter that is constant and known as the stability and control (or aerodynamics) derivatives
FLC	fuzzy logic control
FOSMC	fuzzy output sliding mode control
FSMC	fuzzy sliding mode control
GA	genetic algorithm
$h$	altitude
$h_e$	command altitude
$I_{\bullet}$	a parameter that is constant and is function of the inertial characteristics of UAV
MOCF	multi objective cost function
MOGA	multi objective genetic algorithm
$N$	the number of rules
$N_{keep}$	the number of kept chromosome for mating
$N^{pop}$	the number of chromosome population
$N^{var}$	the number of chromosome variables
$p$	roll angle rate
PID	proportional, integral and derivative
$Q$	pitch angle rate
$R$	yaw angle rate
$r_i$	relative degree of system
$s$	sliding function
$S$	sliding surface
$s_{low}$	fuzzy input variable lower boundary
$S_m$	linguistic value of fuzzy input variable ( $s$ )
$s_{up}$	fuzzy input variable upper boundary
SMC	sliding mode control
$U$	forward velocity
$u_{low}$	fuzzy output variable lower boundary
$U_m$	linguistic value of fuzzy output variable ( $\delta_E$ )
$u_{up}$	fuzzy output variable upper boundary
UAV	unmanned aerial vehicle
$V$	lateral velocity
$V_t$	total velocity
$W$	vertical velocity
<b>X</b>	state vector
$X_1$	state vector of longitudinal channel
$X_2$	state vector of lateral-directional channel
<b>Y</b>	output vector
$Y_c$	desired output vector
$\lambda_{iy}$	a constant number
$\eta$	a constant number
$\delta_E$	elevator control variable

$\delta_R$	rudder control variable
$\delta_A$	aileron control variable
$\phi$	roll angle
$\theta$	pitch angle
$\psi$	heading angle
$\phi_c$	command heading angle
$\alpha$	command roll angle
$\alpha$	angle-of-attack
$\beta$	side slip angle
$\sigma$	the standard deviation of the normal distribution
$\xi$	damping ratio
$\omega_n$	natural frequency
$\mu_A(x)$	MF (membership function) of $A$ set at $x$ value

## 1.0 INTRODUCTION

Autonomous unmanned aerial vehicles (UAVs) have become increasingly attractive for mission where human presence is dangerous or difficult. UAVs have demonstrated various civil and military applications such as urban traffic control, communication relay, border patrol, and battlefield deployment. Among many issues in the development of autonomous UAVs, the modelling and autopilot design are important tasks. In practice, the dynamic of UAVs is nonlinear, time varying, and uncertain; this may lead to performance degradation. Therefore, one of the major problems in designing autopilot is to regard the uncertainties such as parameters variations and unknown nonlinear dynamics. These uncertainties have been driven the researchers to robust methods.

In this paper, the altitude hold mode autopilot is planned for an UAV which is aerodynamically controlled by the elevator control surface, and the considered uncertainties are due to both parametric uncertainties and un-modelled nonlinear terms. This mode is practically important for unmanned aerial vehicles due to flying in vicinity of terrain by terrain following maneuver in a wide range of altitudes. The altitude hold mode is used to maintain a reference altitude which is specified by the trajectory planning algorithm. In linear procedure of the altitude hold mode autopilot design, it is assumed that the longitudinal and lateral-directional motions are independent. But, for non-zero roll angle in turn manoeuvres, this assumption is not valid because decreasing the lift force leads to decreasing the altitude. This effect is based on the nonlinear behaviour of UAVs. Although the altitude hold mode reacts with respect to this effect, it is still necessary to compensate furthermore in order to obtain desirable performances in presence of nonlinear effects. In Refs 1-4, UAV altitude has been controlled. The altitude hold mode autopilot has been designed based on the uncertain linear model in Refs 1-3, and based on the uncertain nonlinear model in Ref. 4. In Ref. 4, the desirable autopilot has been achieved by combination of the classic control and the conventional fuzzy logic control (FLC). The classic controller is considered as a principal section of autopilot, and FLC is used to increase the robustness. Here, it is tried to follow the problem and general procedure in Ref. 4.

Most nonlinear methods such as the feedback linearisation and the sliding mode control<sup>(5)</sup> are heavily based on the knowledge of vehicle mathematical model, and these methods cannot also handle the non-minimum phase systems such as the altitude (output) to elevator (input) dynamic. Here, in order to get rid of the exact model restrictions, FLC is applied to design the robust altitude autopilot because fuzzy logic control does not require accurate model of UAV. The

previous researches<sup>(2-4,6-13)</sup> show that the fuzzy logic control gives desirable performance in terms of time response characteristics and robustness with respect to the uncertainties in parameters and un-modeled dynamics. This is a significant advantage because achieving an accurate mathematical model that is associated with uncertainties is difficult, time-consuming, and expensive (for example, the wind tunnel tests to obtain the aerodynamic coefficients are time-consuming and expensive).

Although the conventional fuzzy logic control is very promising for several applications, they suffer two main problems:

1. The long computational time because of complex decision making processes due to the large set of rules and
2. Incapability of stability analysis.

As the purpose of this paper, we are going to take advantage of FLC together minimising computational burden and increasing capability of stability analysis as follows:

1. For solving the first problem, the fuzzy sliding mode control (FSMC) is proposed. The FSMC can reduce the conventional two-inputs FLC (error and error rate) to a single-input FLC (sliding function). Therefore, FSMC offers significant reduction in rule inferences then control parameters (reduction in number of inputs leads to considerable reduction in the number of rules). This simplification leads to reduction the computational burden and closing to the practical autopilot. Also, the processing time of controller optimisation and complexity will be reduced. FSMC method has recently been used for various applications, such as Refs 14-21. Furthermore, the discouraging problem beside FSMC is defining the sliding surface based on the state vector. In this situation, measurement of several variables and observer are required. Defining the sliding surface based on the outputs leads to the simple fuzzy sliding mode control entitled fuzzy output sliding mode control (FOSMC)<sup>(18)</sup>. Thus, according to these discussions, we exploit FOSMC as the proposed method to design altitude hold mode autopilot.
2. For solving the second problem, similar to Refs 1 and 4, the classic controller is initially designed based on the nominal linear model. It is expected that the closed-loop performance is desirable in absence of uncertainties. In the next step, for improving the robustness with respect to the uncertainties, FOSMC is accompanied with the classic controller. According to this method, we have the two-section controller: classic controller as the major section (with stability analysis capability) and FOSMC (with simple implementation and robustness improving capability).

Designing fuzzy systems requires sufficient experience and expertness. In this case, it is necessary to use/provide an automatic tool for optimal design of fuzzy systems. In recent years, evolutionary algorithms (EAs) have been demonstrated as a suitable alternative technique for optimization of fuzzy systems so that they have been widely used in different applications<sup>(4,8-13)</sup>. In Refs 8 and 12, the missile acceleration that includes non-minimum phase property has been indirectly controlled (lateral velocities are controlled) by FLC and a multi-objective GA. In Ref. 9, the GA-based fuzzy PID controller has been presented to eliminate undershoot of non-minimum phase linear systems. In Ref. 10, a GA-based fuzzy logic controller has been designed to stabilise satellite attitude. Here, the multi-objective genetic algorithm (MOGA) is used to mechanise the optimal determination of FOSMC parameters as well. The objectives include undershoot, overshoot,

rise time, settling time, steady state error and stability. We expect that the solution derived based on this MOGA is desirable because of considering various time-response criteria.

The rest of the paper is organised as follows: Section 2 presents the nonlinear and linear model of the UAV. The proposed strategy will be discussed in Section 3. After the simulation of the proposed strategy, several results are presented in Section 4. Finally, conclusions are drawn in Section 5.

## 2.0 UNMANNED AERIAL VEHICLE MODEL

The UAV equations of motion can be separated into rotational and translational equations. The rotational motion of UAV is equivalent to yaw, pitch, and roll motions about the centre of mass. Other components of the motion are translation of centre of mass in 3D space. Therefore, the UAV model used here will be a six-degree-of-freedom model<sup>(22)</sup>. We utilise the derived nonlinear and linear model in Ref. 4, as follows.

### 2.1 Nonlinear model

$$\dot{U} = RV - QW - g \sin\theta + C_{xU}U + C_{x\alpha}\alpha + C_{xQ}Q + C_{x\delta_E}\delta_E + F_{x0} \quad \dots (1)$$

$$\dot{V} = PW - RU + g \sin\phi \cos\theta + C_{y\beta}\beta + C_{yP}P + C_{yR}R + C_{y\delta_A}\delta_A + C_{y\delta_R}\delta_R \quad \dots (2)$$

$$\dot{W} = QU - PV + g \cos\phi \cos\theta + C_{zU}U + C_{z\alpha}\alpha + C_{zQ}Q + C_{z\delta_E}\delta_E + F_{z0} \quad \dots (3)$$

$$\dot{P} = I_1PQ + I_2QR + C_{L\beta}\beta + C_{LP}P + C_{LR}R + C_{L\delta_A}\delta_A + C_{L\delta_R}\delta_R \quad \dots (4)$$

$$\dot{Q} = I_3PR + I_4(R^2 - P^2) + C_{MU}U + C_{M\alpha}\alpha + C_{MQ}Q + C_{M\delta_E}\delta_E + M_0 \quad \dots (5)$$

$$\dot{R} = I_5PQ - I_1QR + C_{N\beta}\beta + C_{NP}P + C_{NR}R + C_{N\delta_A}\delta_A + C_{N\delta_R}\delta_R \quad \dots (6)$$

$$\dot{\alpha} = \frac{\dot{W} \cos\alpha - \dot{U} \sin\alpha}{V_t \cos\beta} \quad \dots (7)$$

$$\dot{\beta} = \frac{1}{V_t} [-\dot{U} \cos\alpha \sin\beta + \dot{V} \cos\beta - \dot{W} \sin\alpha \sin\beta] \quad \dots (8)$$

$$\dot{\phi} = P + Q \sin\phi \tan\theta + R \cos\phi \tan\theta \quad \dots (9)$$

$$\dot{\theta} = Q \cos\phi - R \sin\phi \quad \dots (10)$$

$$\dot{\psi} = (Q \sin\phi + R \cos\phi) \sec\theta \quad \dots (11)$$

$$\dot{h} = V_t \sin\gamma \quad \dots (12)$$

$$V_t = \sqrt{U^2 + V^2 + W^2} \quad \dots (13)$$

$$\gamma = \theta - \alpha \quad \dots (14)$$

**Table 1**  
**The constants in Equations (1)-(6)**

$g$	$I_1$	$I_2$	$I_3$	$I_4$	$I_5$	$C_{xU}$	$C_{x\alpha}$	$C_{xQ}$
$9.8 \text{ ms}^{-2}$	0.04	-1.51	1.03	0.017	-0.85	$\frac{-0.0125}{\text{s}^{-1}}$	$-16.6 \text{ ms}^{-2}$	$0 \text{ ms}^{-1}$
$C_{x\delta_E}$	$F_{x0}$	$C_{zU}$	$C_{z\alpha}$	$C_{zQ}$	$C_{z\delta_E}$	$F_{z0}$	$C_{MU}$	$C_{M\alpha}$
$16.6 \text{ ms}^{-2}$	$4.5 \text{ ms}^{-2}$	$-0.068 \text{ s}^{-1}$	$-259 \text{ ms}^{-2}$	$-1.3 \text{ ms}^{-1}$	$57.5 \text{ ms}^{-2}$	$21 \text{ ms}^{-2}$	$0 (\text{ms})^{-1}$	$-988 \text{ s}^{-2}$
$C_{MQ}$	$C_{M\delta_E}$	$M_0$	$C_{y\beta}$	$C_{yP}$	$C_{yR}$	$C_{y\delta_A}$	$C_{y\delta_R}$	$C_{L\beta}$
$-8.9 \text{ s}^{-1}$	$1362 \text{ s}^{-2}$	$-0.284 \text{ s}^{-2}$	$-264 \text{ ms}^{-2}$	$-0.0053 \text{ ms}^{-1}$	$1.64 \text{ ms}^{-1}$	$\frac{-0.0032}{\text{ms}^{-2}}$	$-58.2 \text{ ms}^{-2}$	$76.7 \text{ s}^{-2}$
$C_{LP}$	$C_{LR}$	$C_{L\delta_A}$	$C_{L\delta_R}$	$C_{N\beta}$	$C_{NP}$	$C_{NR}$	$C_{N\delta_A}$	$C_{N\delta_R}$
$-1.9 \text{ s}^{-1}$	$-0.68 \text{ s}^{-1}$	$149 \text{ s}^{-2}$	$105 \text{ s}^{-2}$	$306 \text{ s}^{-2}$	$-0.044 \text{ s}^{-1}$	$-2.82 \text{ s}^{-1}$	$2.27 \text{ s}^{-2}$	$434 \text{ s}^{-2}$

where,  $I_i$ 's and  $C_{ij}$ 's are respectively inertial properties and stability and control derivatives of the UAV that their values are presented in Table 1. These equations are nonlinear and highly coupled. Concerning Equations (1)-(14), there is coupling between the lateral-directional channel and the longitudinal channel that will be canceled in the linearisation procedure. For example, in turn manoeuvre, the lift force then the altitude is decreased due to non-zero roll angle. This effect is cancelled during the linearisation process. Nonlinearity may cause performance degradation of the nominal linear model-based autopilot after applying it to the nonlinear model.

## 2.2 Nominal linear model

$$\frac{h(S)}{\delta_e(S)} = \frac{-57 \cdot 3 (S - 24.6)(S + 21)(S + 0 \cdot 008)}{(S^2 + 0 \cdot 011S + 0 \cdot 0022)(S^2 + 2 \cdot 12S + 98 \cdot 4)} \quad \dots (15)$$

The nominal linear model is considered as the available mathematical model that the autopilot is designed based on it. Concerning Equation (15), it is obvious that the altitude output and the elevator input relation is non-minimum phase. This is a fact for altitude-elevator dynamics of aircrafts.

## 2.3 Degraded linear model

$$\frac{h(S)}{\delta_e(S)} = \frac{-57 \cdot 3 (S - 25 \cdot 8)(S + 21 \cdot 75)(S + 0 \cdot 000013)}{S(S^2 + 0 \cdot 004S + 0 \cdot 0021)(S^2 + 1 \cdot 73S + 54)} \quad \dots (16)$$

The degraded linear model is considered to investigate the parametric robustness. Degraded linear model has been derived by applying 50% error in the effective stability derivatives. Reduction in the effective stability derivatives causes moving an unstable zero further to the right, and degradation of both phugoid and short period flight modes.

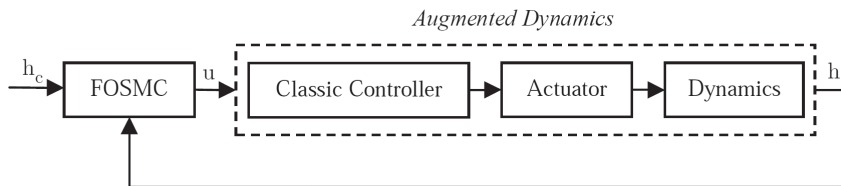


Figure 1. The proposed strategy scheme based on the combination of FOSMC and classic controller.

### 3.0 ALTITUDE HOLD MODE AUTOPILOT DESIGN (PROPOSED STRATEGY)

In this section, the proposed strategy to design the altitude autopilot of the UAV is discussed as follows.

1. The classic control methods include advantages such as the capability of stability analysis and simplicity of implementation. For these reasons, the classic methods have practical interests in automatic flight control systems. Therefore, autopilot is initially designed by using classic methods based on the nominal linear model herein. This autopilot can be desirable in absence of uncertainties and nonlinearities.
2. The sliding mode control (SMC) is a robust design methodology using a systematic scheme based on a sliding mode surface and Lyapunov stability theorem. The main advantage of SMC is that the system uncertainties and external disturbances can be handled under the invariance characteristics of system's sliding mode state with guaranteed system stability. One of major problem associated with SMC is dependency on the plant mathematical model. Conjunction of SMC concept and FLC can help to introduce FSMC that is independent of the plant model. Fuzzy systems are knowledge-based or rule-based systems. The heart of a fuzzy system is knowledge consisting of the so-called fuzzy IF-THEN rules. A fuzzy IF-THEN rule is an IF-THEN statement in which some words are characterized by proper membership functions. As a disadvantage, it is known that the stability analysis of FLC is difficult and insecure while it can be accomplished for model-based procedures.
3. Based on the above discussions, fuzzy output sliding mode control is proposed to improve the basic autopilot (the classic controller) performance. FOSMC is independent of the plant model, is a single input fuzzy system, and is based on the system output. Consequently, the efficient strategy is proposed to design the altitude hold mode autopilot by combination of classic control and FOSMC. In Fig. 1, this strategy is illustrated while  $u$  is the contribution of FOSMC in control of the UAV augmented with classic controller.

In short, the presented strategy has some advantages comparing to the conventional FLC:

1. The controller includes considerable low number of rules because of presence of single input-single output FOSMC. This leads to considerable reduction in computational time.
2. The controller has two portions: (A) classic controller with stability analysis capability and (B) FOSMC without stability analysis capability. The classic controller is the principal portion of controller. In absence of uncertainties and nonlinearities, the role of FOSMC is low while in presence of them, the contribution of FOSMC is highlighted.

### 3.1 Fuzzy output sliding mode control

SMC theory uses discontinuous control action to drive state trajectories toward a specific surface (sliding surface) until stable equilibrium states are reached (5). This principle provides guidance to design a fuzzy logic controller.

Consider the following  $n$ th order nonlinear system:

$$\begin{aligned}\dot{\mathbf{X}}(t) &= \mathbf{F}(\mathbf{X}) + \mathbf{G}(\mathbf{X})\mathbf{U} \\ \mathbf{Y}(t) &= \mathbf{C}(\mathbf{X})\end{aligned}\quad \dots (17)$$

where  $\mathbf{X} = [x_1, x_2, \dots, x_n]^T$  is the state vector, and  $\mathbf{U}$  is the control input. If the desired output vector is defined as  $\mathbf{Y}_c = [y_{c1}, y_{c2}, \dots, y_{cl}]^T$ , then the output error vector  $\mathbf{E} = [e_1, e_2, \dots, e_l]^T$  can be written as follows.

$$\mathbf{E} = \mathbf{Y} - \mathbf{Y}_c = [y_1 - y_{c1} \quad y_2 - y_{c2} \quad \dots \quad y_l - y_{cl}]^T \quad \dots (18)$$

A linear function entitled sliding function  $s : \mathbb{R}^l \rightarrow \mathbb{R}^l$  is defined as

$$\mathbf{s} = \Phi(d/dt)\mathbf{E} \quad \dots (19)$$

where

$$\Phi(d/dt) = \text{diag}[D_1(d/dt), D_2(d/dt), \dots, D_l(d/dt)] \quad \dots (20)$$

In this equation,  $D_i(d/dt)$  is linear function of derivative operators  $\frac{d^{n-1}}{dt^{n-1}}, \frac{d^{n-2}}{dt^{n-2}}, \dots, \frac{d}{dt}$  as following equation.

$$D_i(d/dt) = \lambda_{i,1} \frac{d^{r_i-1}}{dt^{r_i-1}} + \lambda_{i,2} \frac{d^{r_i-2}}{dt^{r_i-2}} + \dots + \lambda_{i,r_i-1} \frac{d^{r_i-(r_i-1)}}{dt^{r_i-(r_i-1)}} + \lambda_{i,r_i} \quad \dots (21)$$

where,  $\lambda_{iy}$  is a constant that can lead to a stable dynamic. Based on these definitions, the sliding surface can be represented as follows.

$$\mathbf{S} = \Phi(d/dt)\mathbf{E} = 0 \quad \dots (22)$$

To design the control input  $U(t)$  so that the output trajectories are driven and attracted toward the sliding surface and then remain on it, the following inequality must be satisfied.

$$\mathbf{s}^T \dot{\mathbf{s}} < -\eta \|\mathbf{s}\| \quad \dots (23)$$

The idea behind Equation (23) is in the sense of Lyapunov function. If we treat  $s$  as a scalar function and the Lyapunov function  $v$  is defined as Equation (24), together with (23), we can ensure that the asymptotic stability of the system is guaranteed.

$$v = \frac{1}{2} \mathbf{s}^T \mathbf{s} > 0 \quad \dots (24)$$

Because we concern on the altitude control, Equations (1)-(12) can be re-written as follows.

$$\begin{aligned} \dot{\mathbf{X}} &= \mathbf{F}(\mathbf{X}) + \mathbf{G}(\mathbf{X})\mathbf{U} \\ \mathbf{Y} &= h \\ \ddot{h} &= f(\mathbf{X}_1) + g(\mathbf{X}_1)\delta_1 + \Delta(\mathbf{X}_2, \delta_2) \end{aligned} \dots (25)$$

where  $\mathbf{X} = [\mathbf{X}_1^T \ \mathbf{X}_2^T]^T$ ,  $\mathbf{X}_1 = [U \ W \ Q \ \theta \ \alpha]$ ,  $\mathbf{X}_2 = [V \ P \ R \ \phi \ \beta]^T$ ,  $\mathbf{U} = [\delta_1^T \ \delta_2^T]^T$ ,  $\delta_1 = \delta_E$ ,  $\delta_2 = [\delta_A \ \delta_R]^T$ . In this equation,  $\Delta(\mathbf{X}_2, \delta_2)$  called the coupling term is contribution of lateral-directional variables. Specially, the term  $\Delta$  is nearly zero when  $\psi_c$  and  $\phi_c$  are zero. Besides,  $\mathbf{F}(\mathbf{X})$ ,  $f(\mathbf{X}_1)$ ,  $\mathbf{G}(\mathbf{X})$ , and  $g(\mathbf{X}_1)$  are the continuous linear or the nonlinear functions that are derived by using Equations (1)-(12).

According to Equation (25), the sliding function is defined as the following equation ( $r_i = 2$  and  $l = 1$ ):

$$s = \lambda e + \dot{e} \dots (26)$$

Where,  $e = -h_c$  is tracking error in the control loop. Based on Equation (26), the sliding surface is presented as follows:

$$S = \lambda e + \dot{e} = 0 \dots (27)$$

By concerning the Equations (23) and (25), we have the following Equation.

$$\begin{aligned} s\dot{s} &= s[\lambda\dot{e} + \ddot{e}] \\ &= s(f(\mathbf{X}_1) + \Delta(\mathbf{X}_2, \delta_2)) + g(\mathbf{X}_1)s\delta_E - s\ddot{h}_c + \lambda s\dot{e} \\ &\leq |s|F_0 + g(\mathbf{X}_1)s\delta_E - s\ddot{h}_c + \lambda s\dot{e} \end{aligned} \dots (28)$$

where, the coupling term is assumed to be bounded by some known function ( $|f(\mathbf{X}_1) + \Delta(\mathbf{X}_2, \delta_2)| \leq F(\mathbf{X})$ ). Based on Equations (23) and (28), the following inequality must be satisfied.

$$|s|F + g(\mathbf{X}_1)s\delta_E - s\ddot{h}_c + \lambda s\dot{e} < -\eta|s| \dots (29)$$

By focusing on the left-hand side second-term of the inequality (29), we can achieve the following results:

1. The control input on the two sides of the sliding surface are opposite in sign and its magnitude is proportional to the sliding function (26).
2. For stability of the system, if the term  $g$  be negative then it is required  $sign(\delta_E) = sign(s)$ .

Therefore, we can conclude that  $\delta_E \propto s$  for negative  $g$  (the proportional ratio must be sufficiently large to satisfy the inequality (29)). This discussion can be used to derive FOSMC as the following rule:

$$R_m : IF \ s \ IS \ S_m \ THEN \ \delta_E \ IS \ U_m \dots (30)$$

where  $S_m$  is the linguistic value of  $s$ , and  $U_m$  is the linguistic value of  $\delta_E$  in the  $m$ th -fuzzy rule. Based on this rule, the rules base is presented in Table 2 for FOSMC. Seven membership functions are used to describe input and output; namely, NEGATIVE BIG, NEGATIVE MEDIUM, NEGATIVE SMALL, ZERO, POSITIVE SMALL, POSITIVE MEDIUM and

**Table 2**  
**FOSMC rules**

Rule No.	Rule
1	IF $s$ NB THEN $u$ IS NB
2	IF $s$ NM THEN $u$ IS NM
3	IF $s$ NS THEN $u$ IS NS
4	IF $s$ ZE THEN $u$ IS ZE
5	IF $s$ PS THEN $u$ IS PS
6	IF $s$ PM THEN $u$ IS PM
7	IF $s$ PB THEN $u$ IS PB

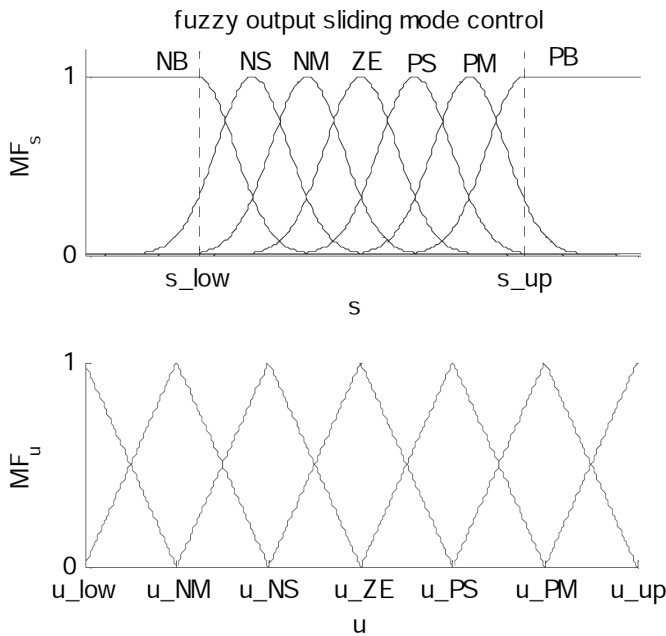


Figure 2. Membership functions for sliding mode function and control variable.

POSITIVE BIG (see Fig. (2)). Here, the Gaussian membership function is used for input (the sliding function).

Suppose that the fuzzy set  $U_m$  and  $S_m$  in (30) are normal with centre  $\bar{u}_m$  and  $\bar{s}_m$ . Then the fuzzy system with rule base (30), product inference engine, singleton fuzzifier, and center average defuzzifier has the following form (23):

$$u = \frac{\sum_{m=1}^M \bar{u}_m \mu_{S_m}(s)}{\sum_{m=1}^M \mu_{S_m}(s)}, \quad \mu_{S_m}(s) = \exp\left[-\left(\frac{s - \bar{s}_m}{2\sigma_m}\right)^2\right] \quad \dots (31)$$

Here,  $M = 7$ .

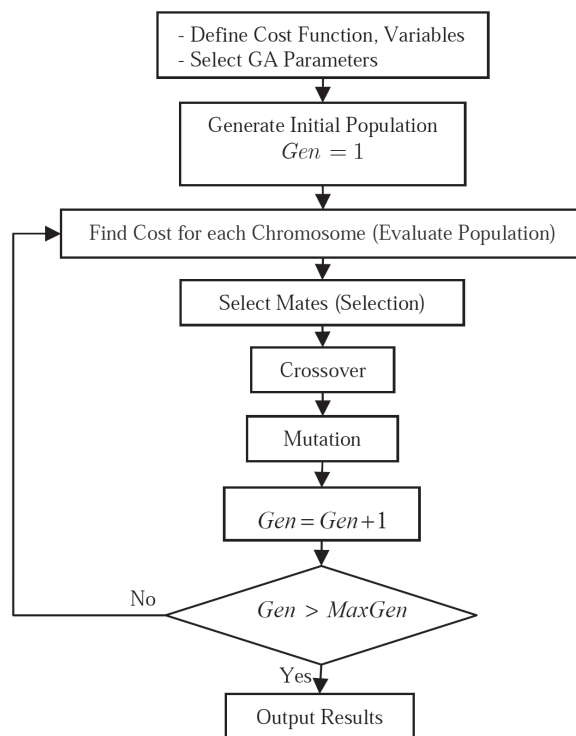


Figure 3. The framework of genetic algorithm.

### 3.2 Optimisation of FOSMC

Conventionally, fuzzy systems are designed by the expert's knowledge and experience. In general, it is difficult to decide about control parameters as the system gets complex. To solve this problem, the determination of FOSMC parameters can be mechanised by GA to comport various criteria such as time response characteristics and robustness.

GA is a search algorithm that is theoretically and empirically proven to provide a robust search in complex spaces. Here, the continuous or real-valued GA is used as following procedure (Fig. 3)<sup>(24)</sup>:

1. Next to defining cost function (fitness function) and design parameters, a chromosome population ( $N_{pop}$ ) is randomly generated.
2. Each chromosome specifies a candidate solution of the optimisation problem. The fitness of all individuals with respect to the optimisation task is then evaluated by the cost function. The cost function generates an output from the set of input variables (the chromosome). The object is to modify the output in some desirable fashions by finding the appropriate values for the input variables.
3. If the chromosome has  $N_{var}$  variables given by  $p_1, p_2, \dots, p_{N_{var}}$ , then the chromosome is written as an  $N_{var}$  element row vector. Now, it is the time to decide which chromosomes in the initial population are fit enough to survive and possibly reproduce offspring in the next generation. The  $N_{pop}$  costs and associated chromosomes are ranked from lowest cost to the highest one.

Between the  $N_{pop}$  chromosomes in a given generation, only the top  $N_{keep}$  are kept for mating (process of natural selection) and the rest are discarded to make room for the new offspring.

4. Subsequently, one mother and one father in some random fashions are selected. Each pair produces two offspring (crossover) that contain traits from each parent. A single offspring variable value,  $p_{new}$ , comes from a combination of the two corresponding offspring variable values.
5. If care is not taken, GA can converge too quickly into one region of the cost surface. If this area is in the region of the global minimum, that is good. However, some functions have many local minima. If this tendency to converge quickly is not solved, the local minimum rather than the global minimum is attained. To avoid this problem, it is forced to explore other areas of the cost surface by randomly introducing changes, or mutations, in some of the variables. Most users of the continuous GA add a normally distributed random number to the variable selected for mutation.

For desirable design of FOSMC by GA, presentation of an efficient cost function is of great importance. Defining a proper cost function leads to desirable design for FOSMC. Here, the multi-objective cost function (MOCF) is presented based on the improving undershoot, overshoot, settling time, steady state error, and unstable behaviour as follows:

$$J = w_1 \int_0^{t_1} |h - h_c| dt + w_2 \int_{t_1}^{t_2} |h - h_c| dt + w_3 \int_{t_2}^T |h - h_c| dt \quad \dots (33)$$

where  $w_i$ s are weights for MOCF,  $t_1$  is the time associated with the first intersection of the altitude time response and the step altitude command,  $t_2$  is the time associated with second intersection of the altitude time response and the step altitude command, and  $T$  is the final time of simulation. If the intersections are not created, the  $t_1$  parameter is considered zero. In MOCF (33), the first term covers rise time and undershoot, the second term includes overshoot value, and the third term includes settling time, steady state error, and unstable effects. In this alternative form of the cost function, the computation of all objectives is not individually required, and we can easily consider several important objectives in the simple cost function.

Next to definition of the cost function, the GA-based optimisation of FOSMC is implemented as following procedure:

Due to the computational burden composed by GA, FOSMC is generally evolved off-line based on the available mathematical model of the controlled process. For this reason, the nominal linear model, as the available mathematical model of UAV, is utilised to achieve the FOSMC parameters. Then, by applying the degraded linear model and the nonlinear model in the simulation procedure, the robustness of controller against uncertainties that are not considered in GA is investigated.

## 4.0 AUTOPILOT DESIGN RESULTS

In this section, the proposed strategy is implemented for the UAV presented in Section 2. This work is done in three steps: (1) design and evaluation of classic autopilot, (2) design and evaluation of fuzzy output sliding mode autopilot, and (3) formation of proposed strategy by combination of the results obtained in Step 1 and Step 2 (of course, the FOSMC designed in Step 2 needs re-designing to match with the classic autopilot).

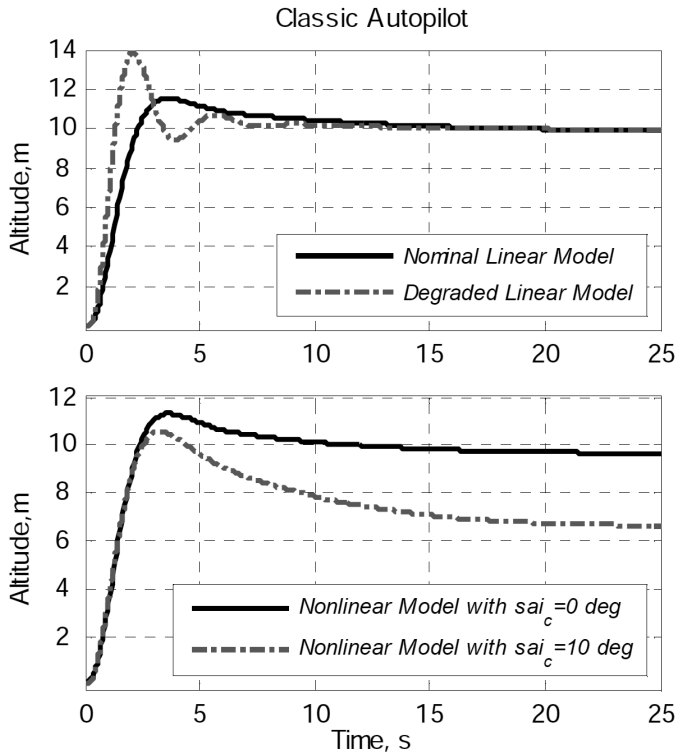


Figure 4. Linear and nonlinear model time response with classic autopilot.

### 4.1 Classic autopilot design

The classic autopilot is designed through the nominal linear model for  $\psi$  and  $h$  variables (the -autopilot that is not presented here has desirable performances, and it is assumed that there are not uncertainties in the directional-lateral channel). By considering a trade-off procedure between the time response characteristics and the robustness, the following compensator is designed through root locus techniques<sup>(4)</sup>.

$$G_C = \frac{0 \cdot 0068(S + 0 \cdot 1) (S^2 + 2 \cdot 12S + 98 \cdot 4)}{(S + 20) (S^2 + 6 \cdot 94S + 13 \cdot 1)} \dots (34)$$

For closed loop system, dominant desirable characteristics are attained by applying this autopilot to nominal linear model (15) as  $\xi = 0 \cdot 79$ ,  $\omega_n = 1 \cdot 36$ . To evaluate this autopilot, it is applied to nominal linear model, degraded linear model and nonlinear model (it should be noted that the elevator trim angle,  $\delta_{Etrim} = 1 \cdot 92^\circ$ , must be added to the control input in the nonlinear simulation procedure because the controllers have been designed based on nominal linear model) then the simulation results are investigated in terms of time response characteristics and robustness. The commands are considered as  $\psi_c = 0$  and 10 degree and  $h_c = 10m$ . The simulation results are illustrated in Fig. 4. Concerning Fig. 4(a), the desirable response is expectantly seen for nominal linear model, but low parametric robustness is obtained for the degraded linear model. By inspection of Fig. 4(b), the time response of classic autopilot has been degraded for the

**Table 3**  
Optimal properties of FOSMC autopilot

$\sigma_{\theta_{NB}}$	$\sigma_{\theta_{NM}}$	$\sigma_{\theta_{NS}}$	$\sigma_{\theta_{ZE}}$	$\sigma_{\theta_{PE}}$	$\sigma_{\theta_{PM}}$	$\sigma_{\theta_{PB}}$	$\bar{u}_{NM}$	$\bar{u}_{NS}$	$\bar{u}_{ZE}$	$\bar{u}_{PS}$	$\bar{u}_{PM}$	$\lambda$
23.6	28.4	16.8	19.8	17.5	26.9	20.8	-7.6	-4.73	0	4.34	9.5	0.84

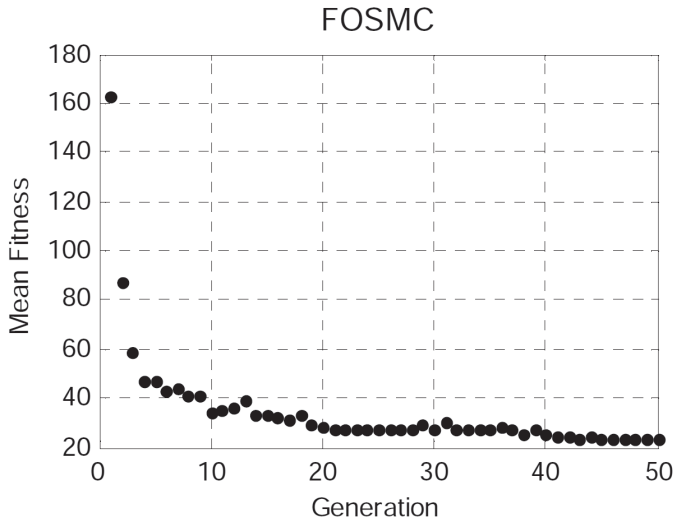


Figure 5. Mean fitness value of generations in evolution of FOSMC autopilot.

UAV nonlinear model because of appearing the nonlinear coupling terms. Clearly, increasing the  $\psi$ -command value (the turn manoeuvre) leads to increasing degraded coupling nonlinear effects (the tendency to lessening altitude). Therefore, in presence of parametric uncertainties and un-modelled dynamics, the compensators cannot meet the requirements. Now, elimination of the nonlinear terms effects is necessary to achieve the desirable tracking. Furthermore, autopilot should not be very sensitive to the variations of system parameters. Due to these reasons, the knowledge-based FOSMC is utilised to overcome the compensator shortcomings.

## 4.2 FOSMC autopilot design

Subsequently, FOSMC is designed by GA. The input variable boundaries are considered as  $s_{up} = 100$ ,  $s_{low} = -100$  and for the output variable, these are  $u_{up} = 12$  deg and  $u_{low} = -12$  deg. Also, the centres of output membership functions ( $\bar{u}_m$ ), variances ( $\sigma_l$ ) of input membership functions, and  $\lambda$  are considered as the chromosome. The GA with the following properties is used to determine the FOSMC parameters:

Chromosome population,  $N_{pop} = 50$

The number of generation = 50

Mutation rate = 2%

$N_{keep} = 50\%$

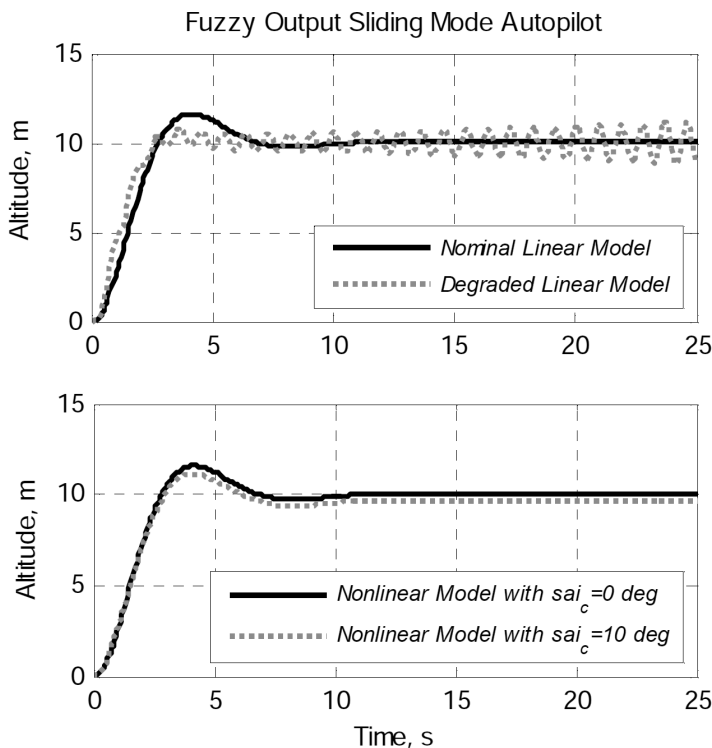


Figure 6. Linear and nonlinear models time response with FOSMC autopilot.

By considering a trade-off procedure between time response characteristics and robustness, the weights are then chosen as  $w_1 = 1$ ,  $w_2 = 1.4$ ,  $w_3 = 1.3$ . The results are presented in Table 3. The mean fitness value in each generation is also shown in Fig. 5.

Simulation results for nominal linear, degraded linear and nonlinear models are shown in Fig. 6. Concerning Fig. 6(a), FOSMC autopilot gives the desirable time response (solid line) and inadequate parametric robustness (dotted line). The desirable nonlinear time response is known in Fig. 6(b) due to eliminating the nonlinear effects. Therefore, the robustness against un-modeled dynamics can be remarkably achieved by the FOSMC autopilot.

### 4.3 Classical and FOSMC autopilot design

Now, it is tried to implement the proposed strategy by combination of the above autopilots. FOSMC associated with the proposed strategy against FOSMC autopilot requires re-designing because of presence of classic controller contribution. The control variable boundaries are chosen  $u_{up} = 30$ ,  $u_{low} = -30$  and these are  $s_{up} = 100$ ,  $s_{low} = -100$  for the sliding function. The weights are considered as  $w_1 = w_2 = w_3 = 1$ , the population size is considered 30, and the other properties of GA are selected similar to FOSMC autopilot. Furthermore, to improve the autopilot performance in the presence of nonlinear effects, Rules 3 and 5 are modified as follows:

**Table 4**  
Optimal properties of the FOSMC in the proposed strategy

$\sigma_{\theta_{NB}}$	$\sigma_{\theta_{NBf}}$	$\sigma_{\theta_{NBg}}$	$\sigma_{\theta_{ZE}}$	$\sigma_{\theta_{PB}}$	$\sigma_{\theta_{PM}}$	$\sigma_{\theta_{PB}}$	$\bar{u}_{NM}$	$\bar{u}_{NS}$	$\bar{u}_{ZE}$	$\bar{u}_{PS}$	$\bar{u}_{PM}$	$\lambda$
16.9	20.9	16.9	22.9	16.2	27.7	17.5	-19.7	-12.3	0	10.7	16.5	2.97

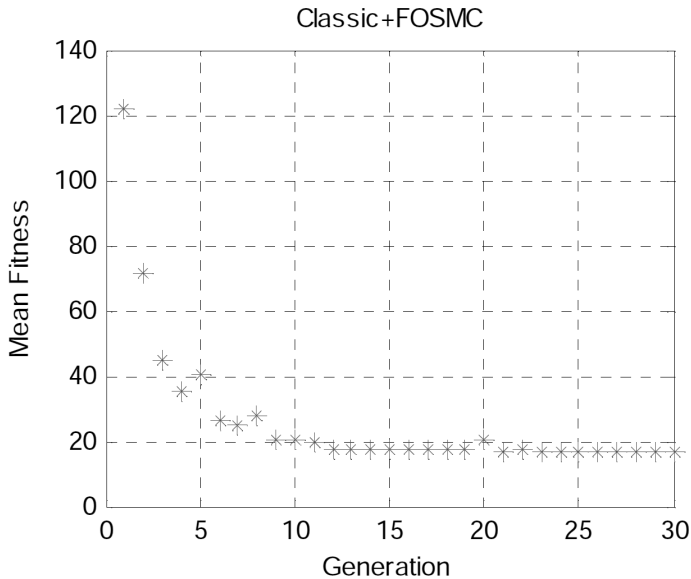


Figure 7. Mean fitness value of generations in evolution of FOSMC in the proposed strategy.

Rule 3: IF  $s$  IS NS, THEN  $L \cdot u$  IS NS, ...

In fact, FOSMC output contribution is multiplied by  $L$  (here, it is chosen 2) to improve the FOSMC performance in presence of the nonlinear coupling effects in the vicinity of command (small sliding function). The GA results based on the UAV nominal linear model are presented in Table 4, and the mean fitness value in each generation is shown in Fig. 7. The simulation results, for the linear and nonlinear model, are illustrated in Fig. 8. This figure displays that the time response characteristics and parametric robustness have been highly improved (Fig. 8(a)). Besides, this strategy leads to the acceptable elimination of nonlinear effects (see Fig. 8(b)).

#### 4.4 Comparison of the autopilots

Subsequently, it is tried to investigate these autopilots in terms of some practical criteria such as effect of the autopilot on other longitudinal variables and the autopilot performance in presence of large commands.

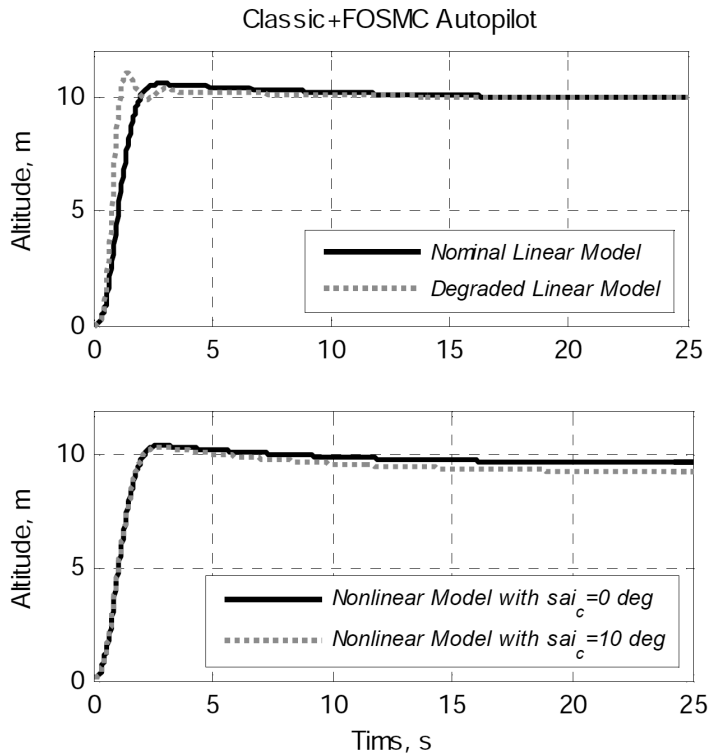


Figure 8. Linear and nonlinear models time response with the proposed autopilot.

**Longitudinal variables:** In the altitude autopilot design procedure, it is required to concentrate on the other longitudinal variables such as pitch angle, pitch rate, and elevator angle because controlling the altitude may lead to degradation of them (altitude variable is important in phugoid mode, and pitch angle and pitch rate are dominant in short period mode). Due to this reason, these variables are illustrated in Fig. 9 for three designed autopilots. As it is clear, the time response of these variables for classic autopilot is better than the others. Classic autopilot has been designed based on improving both short period mode and phugoid mode. Fuzzy output sliding mode autopilot has led to improving only phugoid mode through altitude hold mode autopilot. The proposed strategy not only leads to improving phugoid mode, but also leads to sufficiently improving short period mode because of contribution of classic controller.

**Large commands:** For large commands, it is necessary using a trajectory generation algorithm to avoid the large input and the large load factor. Trajectory generation algorithm leads to constructing a smooth command based on the dynamics limitations. Formation of trajectory generation algorithm is sufficiently complex task. By proper selection of the lower and upper bounds of the FOSMC input and output, the acceptable load factor can be applied to UAV without saturation of the control input. This relaxes us to construct trajectory generation algorithm. According to Fig. 10, the elevator is saturated (the maximum elevator angle is considered 25deg) and the applied load factor is high for classic autopilot due to the large commands (250m). However, FOSMC causes time response to adapt itself with large commands so that the elevator may not be saturated and the applied load factor is acceptable (furthermore, we can

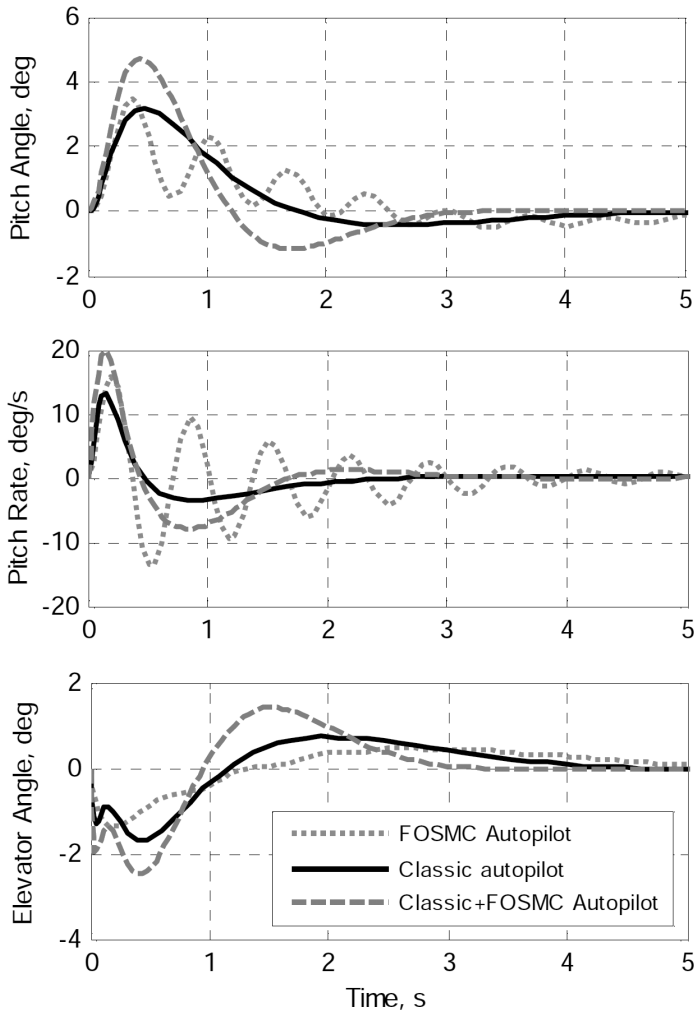


Figure 9. The time response of the dominant variables in the short period mode and control input.

regulate the rate of climb by much focusing on FOSMC parameters). Fortunately, the proposed strategy is better than the fuzzy output sliding mode autopilot in terms of this advantage. In fact, FOSMC confines the control input for large errors, and it returns to the normal conditions for lower errors.

In summary, the three autopilots are compared as follows.

1. The proposed strategy performances are very better than the others in terms of the time response characteristics.
2. The parametric robustness of the proposed strategy is high. This capability depends on the classic controller quality and FOSMC.
3. FOSMC has led to suitable elimination of the coupling nonlinear effects. This capability for FOSMC autopilot is more evident than the proposed strategy.

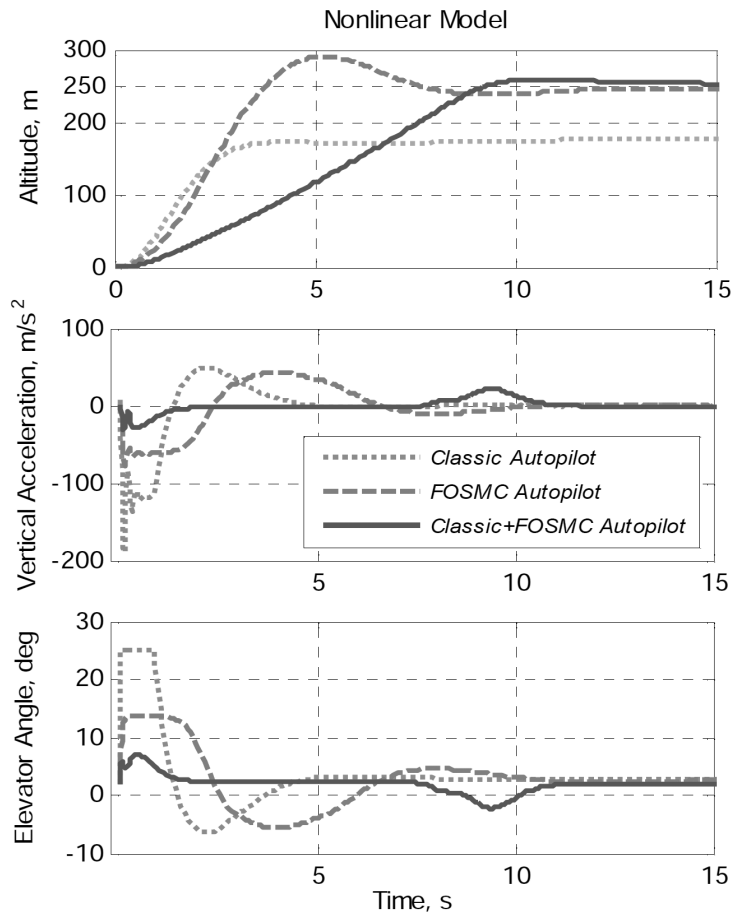


Figure 10. Nonlinear model responses with large command.

4. FOSMC has led to the adaptation of autopilot for large commands so that the control input avoids saturation, and the applied load factor is acceptable. This capability is achieved by proper selection of the boundaries of input and output in FOSMC. Thus, for relatively low errors, proposed strategy provides sufficient inputs for actuator then desirable time response (see Item 1) while the input is limited for large errors because of maximum load factor and elevator requirements.
5. Unlike classic autopilot, FOSMC autopilot is not able to improve short period mode. This is critical for a UAV with weak short period mode. The proposed strategy has improved short period mode by exploitation of the classic controller.
6. GA has mechanised the optimal design of FOSMC. According to Figs 5 and 7, the proposed strategy is evolved in lower generation and lower cost function than FOSMC autopilot. This capability may lead to the evolution of the proposed strategy by an online manner that is an important advantage.
7. Finally, in absence of the uncertainties, classic method is recommended to design the autopilot, and in presence of uncertainties, the presented strategy is proposed.

## 5.0 CONCLUSIONS

In this paper, the combination of classic controller as the principal section of the autopilot and GA-based fuzzy output sliding mode control to increase robustness is applied to the altitude hold mode autopilot for an UAV which is non-minimum phase, and its model includes both the parametric uncertainties and the un-modeled nonlinear terms. The proposed autopilot contains desirable properties: (1) it exploits the classic method with simple implementation and stability analysis capability, and FLC with independency on the system model capability; (2) the processing time composed by FOSMC is lower than the conventional FLC because it is single input fuzzy system; (3) it is based on system output and does not require estimation of system states; (4) optimality of the autopilot is attained by applying the multi-objective genetic algorithm; (5) the simulation results illustrate the capabilities of the proposed strategy in terms of different criteria that are important in practice. Finally, this simple strategy is recommended for the applications that include uncertainties.

## REFERENCES

1. BARKANA, I. Classical and simple adaptive control for non-minimum phase autopilot design, *J Guidance, Control and Dynamics*, 2005, **28**, (4), pp 631-638.
2. BOSSERT, D.E. and COHEN, K. PID and fuzzy logic pitch attitude hold systems for a fighter jet, 2002, AIAA, Guidance, Navigation, and Control Conference and Exhibition, Monterey, CA, USA.
3. COHEN, K. and BOSSERT, D.E. Fuzzy logic non-minimum phase autopilot design, 2003, AIAA, Guidance, Navigation, and Control Conference and Exhibition, 11-14 August 2003, Austin, TX, USA.
4. BABAEI, A.R., MORTAZAVI, M. and MORADI, M.H. Classical and fuzzy-genetic autopilot design for unmanned aerial vehicles, *Applied Soft Computing J*, 2011, **11**, (1), pp 365-372.
5. SLOTINE, J.J.E. and LI, W. *Applied Nonlinear Control*, 1991, Prentice-Hall, Englewood Cliffs, NJ, USA.
6. KADMIRY, B. and DRIANKOV, D. A Fuzzy flight controller combining linguistic and model-based fuzzy control, *Fuzzy Sets and Systems*, 2004, **146**, (4), pp 313-347.
7. WU, S.F., ENGELEN, C.J.H., BABUSKA, R., CHU, Q.P. and MULDER, J.A. Fuzzy logic based full-envelope autonomous flight control for an atmospheric re-entry spacecraft, *Control Engineering Practice*, 2003, **11**, (1), pp 11-25.
8. BLUMEL, A.L., HUGHES, E.J. and WHITE, B.A. Multi-objective evolutionary design of fuzzy autopilot controller, 2001, First International Conference on Evolutionary Multi-Criterion Optimization, pp 668-680.
9. LI, T.H.S. and SHIEH, M.Y. Design of a GA-based PID controller for non-minimum phase system, *Fuzzy Sets and Systems*, 2000, **111**, (2), pp 183-197.
10. OMAR, H.M. Genetic-based fuzzy logic controller for satellites stabilized by reaction wheels and gravity gradient, 2007, AIAA, Guidance, Navigation and Control Conference and Exhibition, Hilton Head, SC, USA.
11. SERRA, G.L.O. and BOTTURA, C.P. Multiobjective evolution based fuzzy PI controller design for nonlinear systems, *Eng Applications of Artificial Intelligence*, 2006, **19**, (2), pp 157-167.
12. TSOURDS, A., HUGHES, E.J. and WHITE, B.A. Fuzzy multi-objective design for a lateral missile autopilot, *Control Engineering Practice*, 2006, **14**, (5), pp 547-561.
13. WU, D. and TAN, W.W. Genetic learning and performance evaluation of interval type-2 fuzzy logic controllers, *Eng Application of Artificial Intelligence*, 2006, **19**, (8), pp 829-841.
14. LIN, C.M. and HSU, C.F. Guidance Law design by adaptive fuzzy sliding-mode control, *J Guidance, Control and Dynamics*, 2002, **25**, (2), pp 248-256.
15. LI, J.H., LI, T.H.S. and OU, T.H. Design and implementation of fuzzy sliding-mode controller for a wedge balancing system, *J Intelligent and Robotics Systems*, 2003, **37**, (3), pp 285-306.
16. LIU, D., YI, J., ZHAO, D. and WANG, W. Adaptive sliding mode fuzzy control for a two-dimensional overhead crane, *Mechatronics*, 2005, **15**, (5), pp 505-522.
17. SEBASTIAN, E. and SOTELO, M.A. Adaptive fuzzy sliding mode controller for the kinematic variables of an underwatervehicle, *J Intelligent and Robotics Systems*, 2007, **49**, (2), pp 189-215.

18. HUANG, Y.J., CHANG, S.H. and KUO, T.C. Robust fuzzy output sliding control without the requirement of state measurement, *J Intelligent and Robotics Systems*, 2008, **53**, (2), pp 169-182.
19. JAFAROV, E.M. and TASALTIN, R. Design of robust autopilot-output integral sliding mode controllers for guided missile systems with parameter perturbations, *Aircraft Eng and Aerospace Tech*, **73**, (1), pp 16-26.
20. SHTESSEL, Y.B., SHKOLNIKOV, I.A. and LEVANT, A. Guidance and control of missile interceptor using second-order sliding mode, *IEEE Transactions on Aerospace and Electronic Systems*, **45**, (1), 2009, pp 110-124.
21. ISHAQUE, K., ABDULLAH, S.S., AYOB, S.M. and SALAM, Z. Single input fuzzy logic controller for unmanned underwater vehicle, *J Intelligent and Robotic Systems*, 2010, **59**, (1), pp 87-100.
22. NELSON, R.C. *Flight Stability and Automatics Control*, 1998, McGraw-Hill.
23. WANG, L.X. *A Course in Fuzzy Systems and Control*, 1997, Upper Saddle River, Prentice-Hall, NJ, USA.
24. HAUPT, R.L. and HAUPT, S.E. *Practical Genetic Algorithm*, 2004, John Wiley & Sons, NJ, USA.